Rose Petal Topography Mimicked Poly(dimethylsiloxane) Substrates for Enhanced Corneal Endothelial Cell Proliferation

M. Özgen Öztürk-Öncel[1], Fatma Zehra Erkoc-Biradli[1], Rıfat Rasier[2], Merve Marçalı[3], Çağlar Elbüken[3,4], Bora Garipcan[1]1

[1]*Institute of Biomedical Engineering, Boğaziçi University, Istanbul, Turkey*

[2]*Department of Ophthalmology, Demiroglu Bilim University, Istanbul, Turkey*

[3]*UNAM-National Nanotechnology Research Center, Institute of Materials Science and Nanotechnology, Bilkent University, Ankara, Turkey*

[4]*Faculty of Biochemistry and Molecular Medicine, Faculty of Medicine, University of Oulu, 90014 Oulu, Finland.*

Highlights

- White rose petal relief topography exhibited CEC microenvironment-like patterns.
- PDMS cell substrates were produced within a cornea-friendly stiffness range.
- COL 4 and HA functionalization of PDMS were characterized.
- Patterned and COL 4 modified PDMS enhanced CEC proliferation, morphology and functionality.

1 Corresponding Author
Boğaziçi University, Institute of Biomedical Engineering, Kandilli Kampus, Uskudar 34684, Istanbul, Turkey
E-mail: bora.garipcan@boun.edu.tr

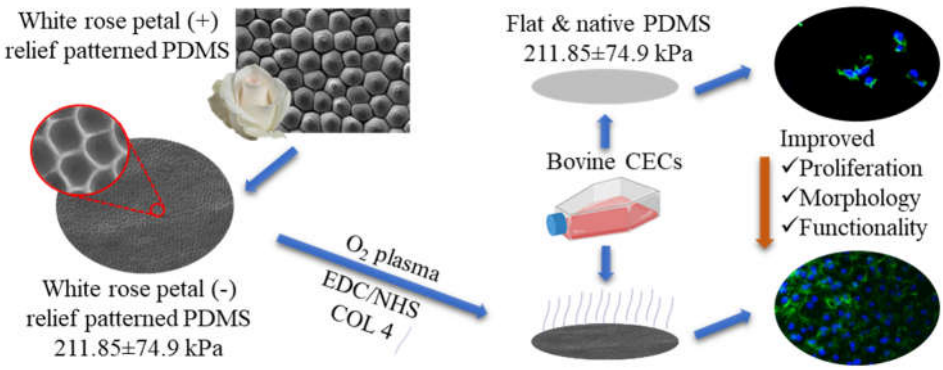

I suggest removing (+) and (-) in the above figure.

Abstract

Low proliferation capacity of corneal endothelial cells (CECs) and worldwide limitations in transplantable donor tissues reveal the critical need of a robust approach for *in vitro* CEC growth. However, preservation of CEC-specific phenotype with increased proliferation has been a great challenge. Here we offer a biomimetic cell substrate design, optimizing mechanical, topographical and biochemical characteristics of CEC microenvironment. We showed the surprising similarity between topographical features of white rose petals and corneal endothelium due to hexagonal cell shapes and physiologically relevant cell density (≈ 2000 cells/mm^2). Polydimethylsiloxane (PDMS) substrates with replica of white rose petal topography and cornea-friendly Young's modulus (211.85±74.9 kPa) were functionalized with two of the important corneal extracellular matrix (ECM) components, collagen IV (COL 4) and hyaluronic acid (HA). White rose petal patterned and COL 4 modified PDMS with optimized stiffness provided enhanced bovine CEC response with higher density monolayers and increased phenotypic marker expression. This biomimetic approach demonstrates a successful platform to improve cell substrate properties of PDMS for corneal applications, suggesting an alternative approach for CEC-based therapies or drug toxicity investigations.

Keywords: Corneal endothelium; Biomimetic cell substrate; White rose petal; Polydimethylsiloxane; Collagen IV; Hyaluronic acid.

1. Introduction

Corneal endothelial cells (CECs) are polygonal-shaped cells and forming monolayer on the posterior surface of the cornea. These cells are specialized for the active pumping of fluids across the cornea to retain its transparency [1]. In young adults, CEC density is ≈ 3000–3500 cells/mm^2, whereas this number decreases throughout lifetime due to the mitotically inactive nature of CECs [2,3]. Trauma, aging, diseases and intraocular surgical procedures accelerate the decay of CEC density. When cell density drops below a critical level (≈ 500 cells/mm^2), endothelial dysfunction occurs, causing the cornea to lose its optical clarity which leads to impaired vision and subsequently to blindness [4,5]. Currently, corneal transplantation or corneal grafts, including full-thickness and selective endothelial keratoplasty are the only treatments for restoring corneal endothelium function [6]. Although these methods are successful, immune reaction and rejection of tissues, in addition to worldwide shortage of transplantable donor corneas hinder their wide-use [7]. Thus, there is a high demand for alternative therapies to repair, replace or regenerate corneal endothelium to overcome CEC loss related visual impairment.

Recent studies on cell-based therapy have provided new opportunities to corneal endothelium replacement by using cell transplantation following an *in vitro* expansion of cells on specific biomaterials [3,8–10]. However, functional expansion of CECs is still a challenge, in addition to their limited potential for *in vitro* proliferation [11,12]. Thus, production of biomaterial platforms for the expansion of CECs in culture environment while preserving their functionalities has been a promising approach. Various natural cell substrates were developed for this purpose, including collagen/ hyaluronic acid/ chitosan [13], chitosan/ polycaprolactone [9,14], cross-linked hyaluronan [15], cross-linked collagen/ gelatin/ hyaluronic acid [16] and decellularized cornea layers [17], but poor mechanical properties and high degradation rates lead to the of synthetic materials [11,18]. On the other hand, synthetic materials lack cell binding cites and therefore they require surface modifications, prior to cell culture.

Nature inspires development of smart structures by mimicking various creatures, like beehives, spider silk networks, gecko feet, shark skin and lotus leaves [19,20]. As natural materials exhibit unique micro- and nanoscale cues with good mechanical performance and biocompatibility, biomimetics was used in cell substrate design as well [21–23]. In native environment, CECs are in direct contact with underlying Descemet's membrane, which is mainly composed of Collagen

type IV (COL 4) and VIII (COL 8) [24]. As the microenvironment of cells and the interaction in between them regulate cellular behavior, properties of Descemet's membrane and corneal extracellular matrix (ECM) have been considered in designing new biomaterials [4,25,26]. Palchesko et al. focused on the chemical and mechanical properties of corneal ECM and prepared polydimethylsiloxane (PDMS) substrates with Descemet's membrane-like mechanical properties. After coating with several ECM proteins, they reported that 50 kPa PDMS with COL 4 coating resulted a significant increase in CEC proliferation, in addition to improved expression of phenotypic markers [4]. Teo et al. developed various micro- and nanoscale geometrical surface patterns (pillars and wells) on PDMS substrates inspired by topographical features of Descemet's membrane. Among them, the nanopillar surface topography was found to be the most suitable pattern to obtain CEC culture with typical cell shape and better functionality [27]. In a similar study, patterned tissue culture polystyrene (TCPS) was confirmed to significantly improve CEC expansion and CEC-related protein expression [12]. A more recent work described the effect of PDMS with Descemet-like surface topography to initiate the differentiation of mesenchymal stem cells (MSC) into corneal endothelial-like cells [28]. Although these studies are inspired by the microenvironment of corneal endothelium, they focused only on one or two important parameters of ECM characteristics. However, combined effects of mechanical, topographical and biochemical properties of cell microenvironment regulate cell behavior *in vivo* and thus a holistic approach is required when designing cell substrates to obtain desired *in vitro*-like cell response [29].

PDMS is a synthetic, non-toxic and optically transparent polymer with adjustable stiffness, surface chemistry and excellent properties for structure replication [30,31]. Here, we developed PDMS cell substrates within the bulk modulus range of cornea [32] and adjusted surface topographical and biochemical properties according to the CEC microenvironment. Young's modulus of 30:1 PDMS base to curing agent ratio was found to be a cornea-friendly stiffness with 211.85±74.9 kPa. Additionally, we took the advantage of naturally occurring patterns - white rose petals (negative reliefs), to control cell substrate topographies. In the literature, red rose petal mimetic/inspired polymer films have been investigated for their superhydrophobic and highly adhesive surface properties [33–35]. The microstructure of rose petals exhibited compactly arranged micropapillae with nanoscaled folds on each micropapillae [36], which may provide a suitable environment for CEC culture. Thus, we examined both red and white rose

petal - mimetic PDMS surfaces and it is to our surprise that the structure of white rose petals is very similar to the natural CEC microenvironment. Inverse reliefs (negative replicate) of white rose petal topographies were used in the PDMS substrate surface design to support cell culture. Furthermore, substrate surfaces were chemically modified with corneal ECM components. Since conventional plasma activation technique provides suitable surfaces for a short duration, we used stable chemical linkages to modify PDMS with either Collagen IV (COL 4) – a predominant collagen in Descemet's membrane [24], or Hyaluronic acid (HA) - an important ECM component of cornea [37]. The combination of these mechanical, topographical and chemical improvements of PDMS substrates enhanced *in vitro* CEC expansion and functional marker expression. This extensive approach can be easily adapted to cornea-on-a-chip applications for drug design or used as a successful cell substrate alternative in corneal cell therapy to decrease the need of donor corneas.

2. Material and methods

2.1.Investigation of cornea-friendly PDMS stiffness

Young's modulus of PDMS substrates with various base and curing agent concentrations (10:1, 15:1, 20:1 and 30:1) were measured using a nanoindenter (CellHesion®200, JPK) in hydrated conditions. Measurements were performed with a CONT cantilever (0.2 N/m force constant and 13 kHz resonance frequency, Nanoworld) in contact mode and 7 samples were analyzed for each type. Young's moduli of different PDMS substrates were calculated according to the Hertz model.

2.2.Preparation of rose topography mimicked PDMS

White (*Rosa Pascali*) and red roses (*Rosa Damascena*) were purchased from a local flower shop. In this study, soft lithography was used to produce rose petal relief negative pattern on PDMS cell substrates. To use the same pattern, the first rose petal relief negative replicate was kept as a mold for casting of successive surfaces. Rose petal topography mimicked negative (-) replica was prepared by mixing 10:1 ratio of PDMS base and curing agent (PDMS, Sylgard 184; Dow). Rigorously stirred mixture was degassed completely and poured onto rose petals. Red and white rose petals were used both in fresh and dried (petals were fixed onto a cork board and allowed to dry under room conditions) form. After 4 h of curing at 70°C, replicas were cleaned by sonicating in DI water, absolute ethanol and DI water, respectively. Both negative and

positive replicas were sputter coated with a thin layer of gold (Quorum SC7640 high resolution sputter coater, 1.5 kV, 10 mA), before using as a mold. 15:1 PDMS base to curing agent ratio was used for the positive (+) replica, as it would be easier to peel off while using PDMS with different base to curing agent ratios. Finally, (white) rose petal topography mimicked cell substrates were prepared with 30:1 PDMS (Section 3.2). This procedure is schematically given in Figure 1. Positive molds supported at least 10 replications (Supporting Information, Figure S1). Mimicked substrates were characterized by a Scanning Electron Microscope (SEM, XL30, Philips) and an optical profilometer (Zygo, CT, USA) for determining morphology and pattern dimensions, respectively.

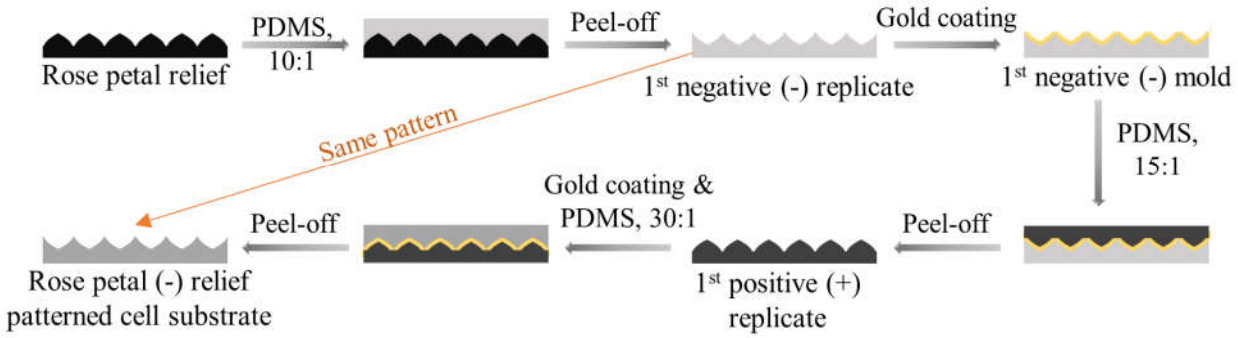

Figure 1. Schematic procedure of rose petal topography mimicked PDMS substrate preparation.

2.3.Surface functionalization of PDMS substrates with COL 4 and HA

PDMS substrate surfaces were modified with COL 4 and HA using EDC/NHS coupling chemistry. First, surfaces were activated via oxygen plasma for 60 s (50 sccm O_2 flow at 200 mTorr pressure, March Plasma Systems) [38] and then they were immersed into 10% (3-aminopropyl)triethoxysilane (APTES) in absolute ethanol to form amine groups (PDMS-NH_2) [38,39]. 1 mg/mL HA (Acros, 251770010) and 0.5 mg/mL COL 4 (Sigma C5533) solutions were prepared in 1:1 EDC and NHS containing MES buffer (50 mM, pH 5.0) and stirred for 30 min [40,41]. Finally, PDMS-NH_2 substrates were incubated in these solutions at room temperature (RT) overnight with subsequent rinsing with MES buffer and DI water (Figure 2).

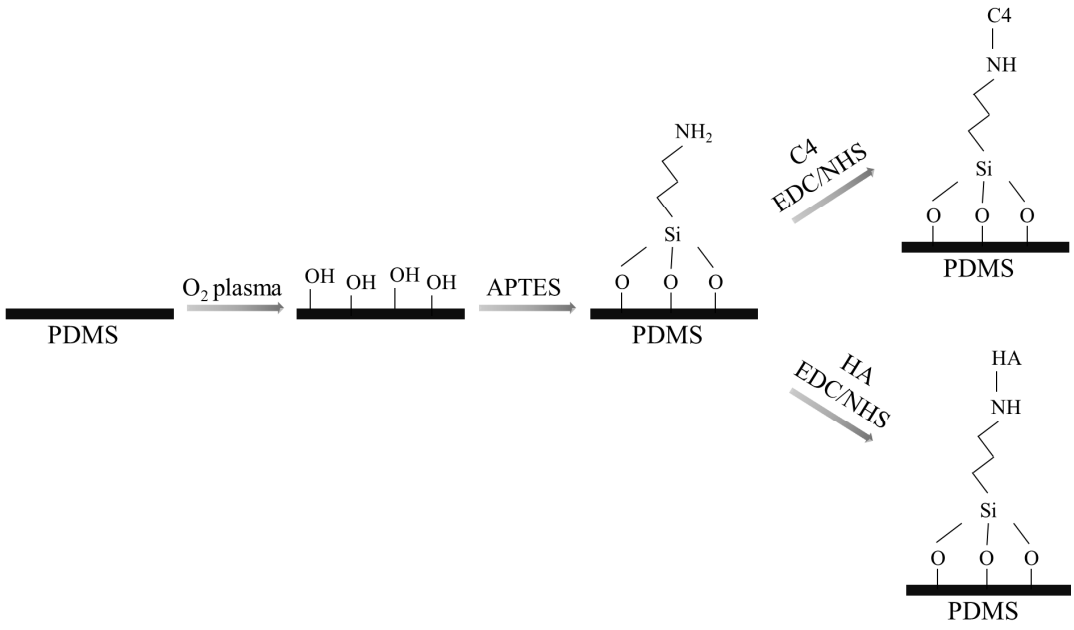

Figure 2. Functionalization of PDMS substrates with COL 4 and HA.

2.4. Characterization of functionalized PDMS substrates

Surface modification of PDMS substrates with COL 4 and HA was confirmed by using water contact angle (WCA) measurements (CAM 100, KSV) with a fixed amount of DI water at RT. In each experimental group, 5 samples were analyzed for their wettability properties.

Changes in surface chemistry after modification were monitored using an X-ray photoelectron spectrophotometer (XPS) with aluminum K-α radiation (Thermo Scientific). 150 eV pass energy was used for the investigation of survey spectra, whereas 50 eV was used for high resolution.

COL 4 and HA functionalization of PDMS substrates were visualized by using immunofluorescent staining. Initially, blocking was performed to eliminate unspecific binding via 22.52 mg/mL glycine containing 1% BSA in PBST (0.1% Tween-20 in PBS) for an hour. Then, substrates were incubated with primary antibodies of anti-collagen IV (ab6586, 1:100) and anti-hyaluronic acid (ab53842, 1:100) in 1% BSA containing PBST overnight at 4°C. After rigorous rinsing of substrates with PBS, secondary antibodies of anti-rabbit IgG H&L (ab150062, Alexa Fluor®555, 1:200) and anti-sheep IgG H&L (ab150177, Alexa Fluor® 488, 1:200) were added to each sample and incubated at RT for an hour. Finally, immunofluorescent

signals were visualized using appropriate excitation filters of a fluorescence microscope (DM IL, Leica).

2.5.Corneal endothelial cell culture

Bovine CECs (BCE C/D-1b, ATCC® CRL-2048™) were cultured on PDMS substrates in 24 well tissue culture plates (TCP) with a density of $1x10^5$ cells/well, using 10% Fetal Bovine Serum (FBS, Merck) supplemented DMEM High glucose with L-Glutamine and Sodium Pyruvate (Biosera). Cells were incubated at 37°C with 5% CO_2 in a humidified environment. PDMS substrates were sterilized before cell culture with 70% ethanol, sterile DI water and UV exposure. CEC cell behavior was investigated on both flat native PDMS (PDMS), COL 4 functionalized PDMS (PDMS-C4), HA functionalized PDMS (PDMS-HA) and white rose petal negative relief topography mimicked versions of these substrates (PDMS-R, PDMS-C4-R and PDMS-HA-R, respectively) with a control group of TCP.

2.6. Cell proliferation assay

Alamar blue assay (AlamarBlue^{TM}, Bio-Rad) was used to investigate CEC proliferation on various PDMS substrates on days 1, 3 and 7. Briefly, cell culture media was removed and 10% alamar blue containing fresh media was added on cells on these specific days. Cells were incubated for 4 h and optical absorbance of each experimental group was recorded on a micro plate reader spectrophotometer (Bio-Rad, iMark) at 570 and 595 nm [31].

2.7. Morphological staining

Cellular morphology on functionalized and white rose petal patterned PDMS substrates was investigated via actin cytoskeleton staining (Alexa Fluor 488 Phalloidin, Thermo Fisher) on the 7^{th} day of CEC culture. Cells were fixed in 4% formaldehyde and permeabilized by immersing into 0.1% Triton X-100 containing PBS. After blocking was completed in 1% BSA for 20 min, actin cytoskeleton staining solution (in 1% BSA) was applied. DAPI counterstaining (Thermo Fisher) was used to visualize cell nuclei. Images were recorded with appropriate filters of a fluorescence microscope (DM IL, Leica) [31].

2.8. Immunocytochemistry

On the 7th day of CEC culture on substrates, cells were fixed and permeabilized as instructed in Section 2.7. Blocking and immunocytochemical staining were performed using the same procedure as in Section 2.4. Anti-sodium potassium ATPase primary antibody (ab76020, EP1845Y, 1:100) and anti-rabbit IgG H&L secondary antibody (ab150062, Alexa Fluor®555, 1:200) were used to label Na^+/K^+ ATPase, and DAPI was used to visualize cell nuclei.

2.9. Western blot analysis

Western blot analyses were performed on the 7th day of CEC culture and expressions of CEC-relative markers Na^+/K^+ ATPase, collagen type IV, N-cadherin and zonula occludens-1 (ZO-1) were investigated on PDMS substrates. Briefly, total proteins were extracted and lysed in 2X Laemmli buffer and equalized amounts of proteins were loaded into 4-10% polyacrylamide gels (Sigma-Aldrich). Then, they were resolved under 130 V (Mini protean, Bio-Rad) and transferred to PVDF membranes (Transblot Turbo, Bio-Rad). After blocking was completed using 5% non-fat milk containing PBST, membranes were incubated with anti-sodium potassium ATPase (ab76020, EP1845Y), anti-collagen IV (ab6586), anti-N-cadherin (ab18203) primary antibodies overnight at 4°C. Anti-β-actin (ab8226) was chosen to be the loading control. On the following day, membranes were rinsed extensively with PBST and incubated with corresponding horseradish peroxidase (HRP)-labeled secondary antibodies (ab6721, and ab6789) for 1 h. 3,3′,5,5′-tetramethylbenzidine chromogenic substrate (Thermo Fisher) was used for the visualization of bands on the membranes and their intensities were calculated using ImageJ.

2.10. Statistical analysis

Graphpad (Prism) software was used to conduct all statistical analyses with one-way analysis of variance (ANOVA) and Tukey multiple comparison test. *p* values lower than 0.05 were regarded as statistically significant. Data were given as mean ± standard deviation (SD).

3. Results

3.1. Topographical features of rose petal mimicked PDMS

Soft lithography was used to transfer rose petal's positive and negative reliefs topographical cues on PDMS substrates. Figure 3A summarizes SEM images of (i) fresh red, (ii) dry red, (iii) fresh white and (iv) dry white rose petal patterned features on 15:1 PDMS surfaces (positive replicas). Herein, both micro- and nano-sized cues were successfully replicated. Due to the

shrinkage of cells in dry petals, cells were disrupted leading to reduced cell number and increased cell-to-cell distances. Therefore, they were not preferred as cell substrates for CECs. In both fresh rose petals patterned ones; cell number is in the range of physiologically relevant CEC density (≈ 2000 cells/mm^2). Microgroove mean depths (N=30 measurements using optical profilometer over 3 PDMS replicas) of the patterned PDMS were calculated to be 12.9 µm (Figure S1) and 6.6 µm (Figure 3C), for red and white rose, respectively. Among them, white rose patterned one ensured CEC-like depth [42]. Furthermore, fresh white rose petal provided better CEC shape-imitative hexagonal cells than red ones. Thus, we used white rose petals (Rosa Pascali) for the fabrication of patterned cell substrates for the remaining experiments. In Figure 3B, SEM images of (i) white rose petal replicating mold and (ii) white rose petal topography mimicked PDMS cell surfaces were given. Highly ordered hexagonal shapes and nano-scale cues in Figure 3A(ii) demonstrated successful replication and CEC shape-imitative cell substrate production.

Replicating capacity of PDMS molds was tested by using a PDMS mold for 10 replications. SEM images of fabricated substrates confirmed that a rose petal patterned PDMS mold could be used at least 10 times without causing any disruptions (Figure S2).

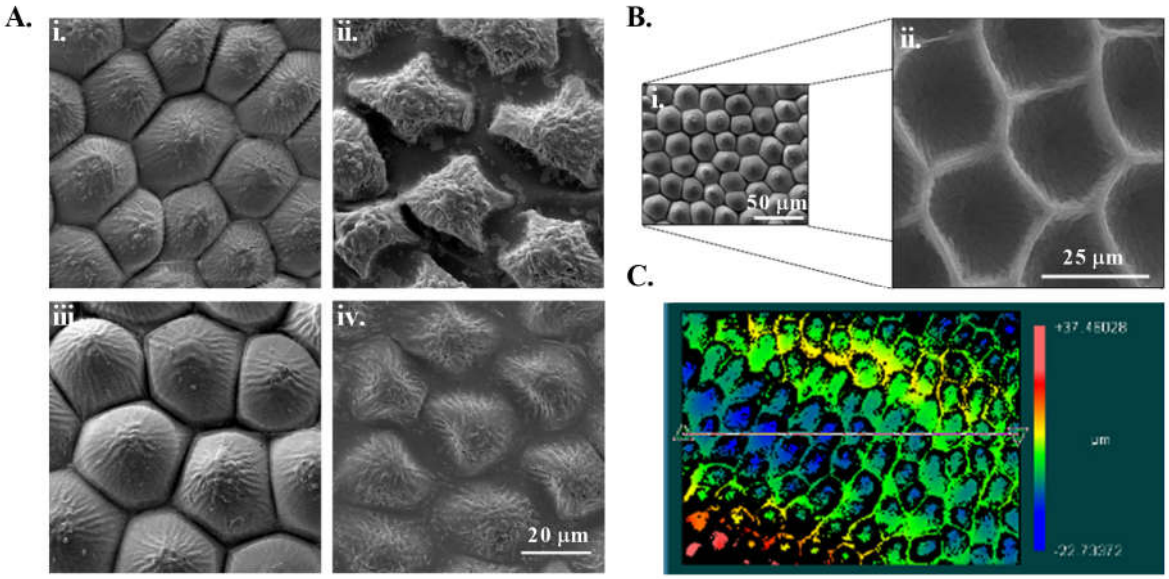

Figure 3. SEM images of rose petal patterns on PDMS surfaces; (A) positive replicas of (i) fresh and (ii) dry red rose, (iii) fresh and (iv) dry white rose petal patterns; (B) fresh white rose

patterned (i) mold and (ii) cell substrate. (C) Surface topography measurements of fresh white rose patterned PDMS.

3.2. Mechanical properties of PDMS substrates

PDMS substrates were prepared in decreasing curing agent concentrations (10:1, 15:1, 20:1 and 30:1) to obtain substrates with a wide stiffness range. Nanoindentation was used for the characterization of these PDMS substrates and Young's modulus values were given in Figure 4A as 2105.3±155.6, 1387.57±152.9, 683.43±188.7 and 211.85±74.9 kPa for 10:1, 15:1, 20:1 and 30:1 PDMS base and curing agent ratios, respectively. All these formulations provided successful pattern replications, whereas lower amounts of PDMS curing agent than 30:1 resulted sticky substrates. The Young's modulus of 30:1 PDMS (211.85±74.9 kPa) was in the cornea-friendly range, which is between 200-290 kPa [32,43–45]. Thus, PDMS with 30:1 base to curing agent ratio was used for the fabrication of all cell substrates.

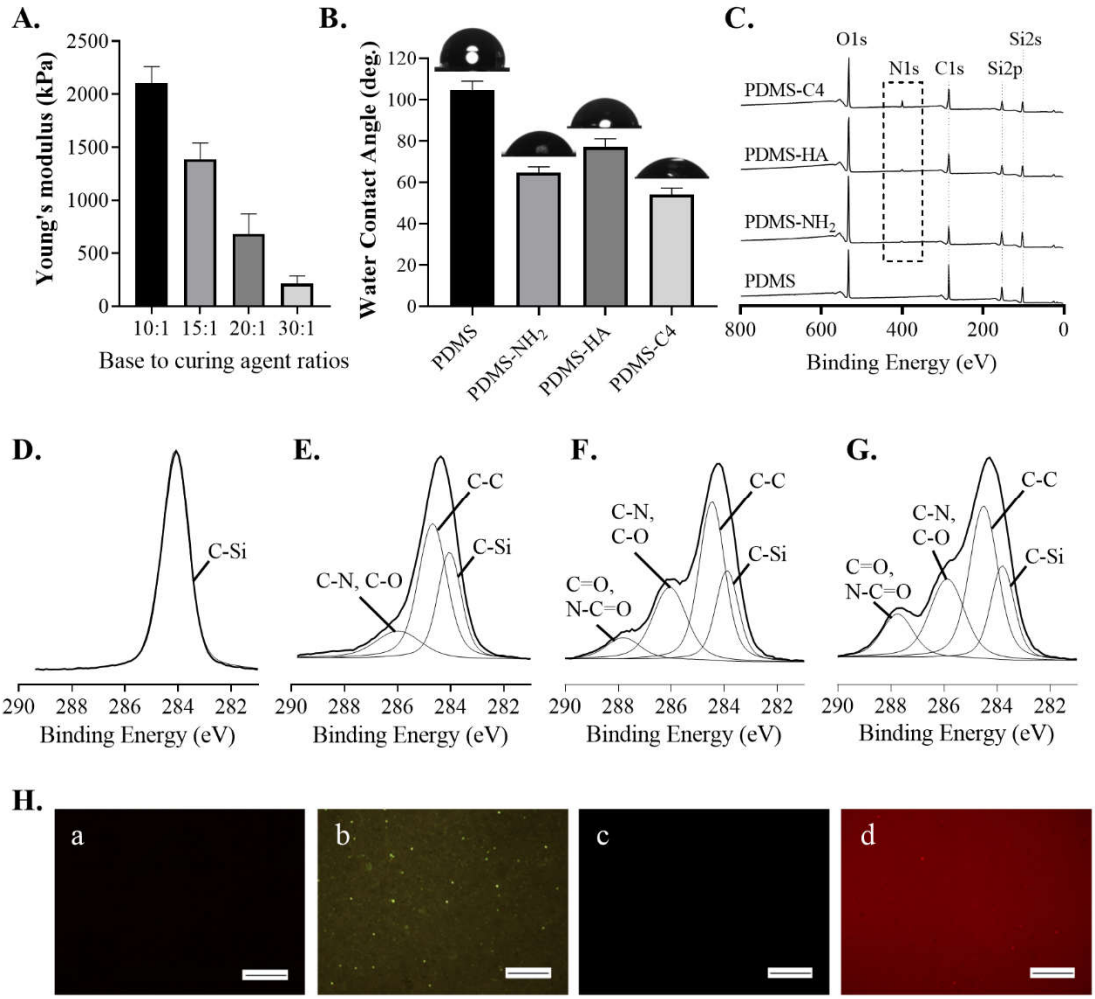

Figure 4. Characterization of PDMS substrates. (A) Nanoindentation measurements of varying PDMS base and curing agent formulations (****$p < 0.0001$); (B) WCA analysis and (C) XPS survey spectra of native PDMS and APTES, HA and COL 4 functionalized PDMS. (D) High resolution C1s spectra of native PDMS, (E) PDMS-NH_2, (F) PDMS-HA and (G) PDMS-C4. (H) Immunofluorescent staining against anti-hyaluronic acid on (i) PDMS and (ii) PDMS-HA; against anti-collagen IV on (iii) PDMS and (iv) PDMS-C4.

3.3.Characterization of PDMS surface functionality

COL 4 and HA functionalization of PDMS substrates were confirmed via WCA measurements for the alteration in surface hydrophobicity, XPS analysis and immunofluorescent staining for surface chemical and biochemical investigation.

Wettability properties of various PDMS substrates were investigated to show the effect of surface functionalization and results are given in Figure 4B. Untreated PDMS surfaces displayed a hydrophobic nature with a water contact angle of 104.6°±4.3°, which was strongly reduced after oxygen plasma treatment and APTES modification (64.7°±2.8°) due to the formation of hydrophilic amine groups. After HA functionalization, PDMS surfaces became more hydrophobic than PDMS-NH_2 with a WCA of 77.2°±3.8°, whereas PDMS-C4 showed the lowest contact angle of 54.1°±3.1°.

XPS survey (Figure 4C) and high resolution spectra were shown (Figure 4D-G) for PDMS, PDMS-NH_2, PDMS-HA and PDMS-C4. In survey spectra, all PDMS related peaks of Si2s, Si2p, C1s and O1s were detected [31]. After modification with APTES, N1s peak was shown at 400.4 eV to confirm the incorporation of $–NH_2$ functional group. When HA or COL 4 were immobilized on PDMS surfaces, there were significant rises in C1s and N1s. This is a clear indication of introducing biomolecules to PDMS surfaces featuring various carbon-nitrogen functionalities. Further investigation was supplied by the high resolution C1s core-level spectra. Four different C species were specified based on their binding energies, C-Si at ≈ 283.7 eV, C-H, C-C at ≈ 284.5 eV, C-N, C-O at ≈ 285.8 eV and N-C=O, C=O at ≈ 287.8 eV [40,46,47]. The appearance of C-C, C-O, and C-N was attributed to the successful chemical modification with APTES, HA and COL 4. Furthermore, the presence of surface amide-type functionalities (N-C=O) confirms the conjugation of PDMS-NH_2 with HA or COL 4.

Immunofluorescent staining was further used to show the uniformity of HA or COL 4 functionalization on PDMS-NH_2 (Figure 4H). No fluorescent signals were observed in native PDMS for both anti-hyaluronic acid and anti-collagen IV staining [Figure 4H(a) and (c)], whereas uniform staining of HA (in green) and COL 4 (in red) were visualized, attributable to the HA or C4 functionalization [40,48].

3.4. *In vitro* growth and morphology of CECs

CEC proliferation and actin cytoskeleton were evaluated on flat and white rose negative relief patterned native, HA functionalized and COL 4 functionalized PDMS surfaces over 7 days. The metabolic activity of CECs on various PDMS substrates was determined via Alamar blue assay on days 1, 3 and 7. The effect of surface chemical modification on CEC proliferation was given in Figure 5A, relative to reduced alamar blue percentages. CEC numbers on all substrates

increase with time. This results verifies the non-toxicity of native and modified PDMS. Among all PDMS substrates, PDMS-C4 enhanced CEC proliferation significantly ($p < 0.0001$) for the whole cell culture period. White rose negative relief patterning of PDMS increased the cell number on all PDMS surfaces (Figure 5B) and with PDMS-C4-R, a TCP-like proliferative environment was achieved for CECs on days 3 and 7. HA functionalization of PDMS did not show any improvements on CEC proliferation relative to native PDMS. Thus, white rose patterning-related cell proliferation was investigated on native and COL 4 modified PDMS (Figure 5C). This effect was clearly visible on day 7 with a statistically increased cell metabolic activity on patterned versions of each group ($p < 0.0001$). In addition to promotive effect of white rose mimicked patterning, COL 4 functionalization resulted an improved CEC bioactivity ($p < 0.0001$).

Cellular morphology on PDMS substrates were investigated on day 7 via actin cytoskeleton staining and fluorescence images of CECs on various surfaces were given in Figure 5D. Very few attached cells were found on flat native PDMS, supporting the proliferation analysis. Both patterning and surface chemical modification increased the number of attached cells on PDMS surfaces. Furthermore, patterned PDMS-C4 provided the most densely CECs population with well-defined actin fibers organization.

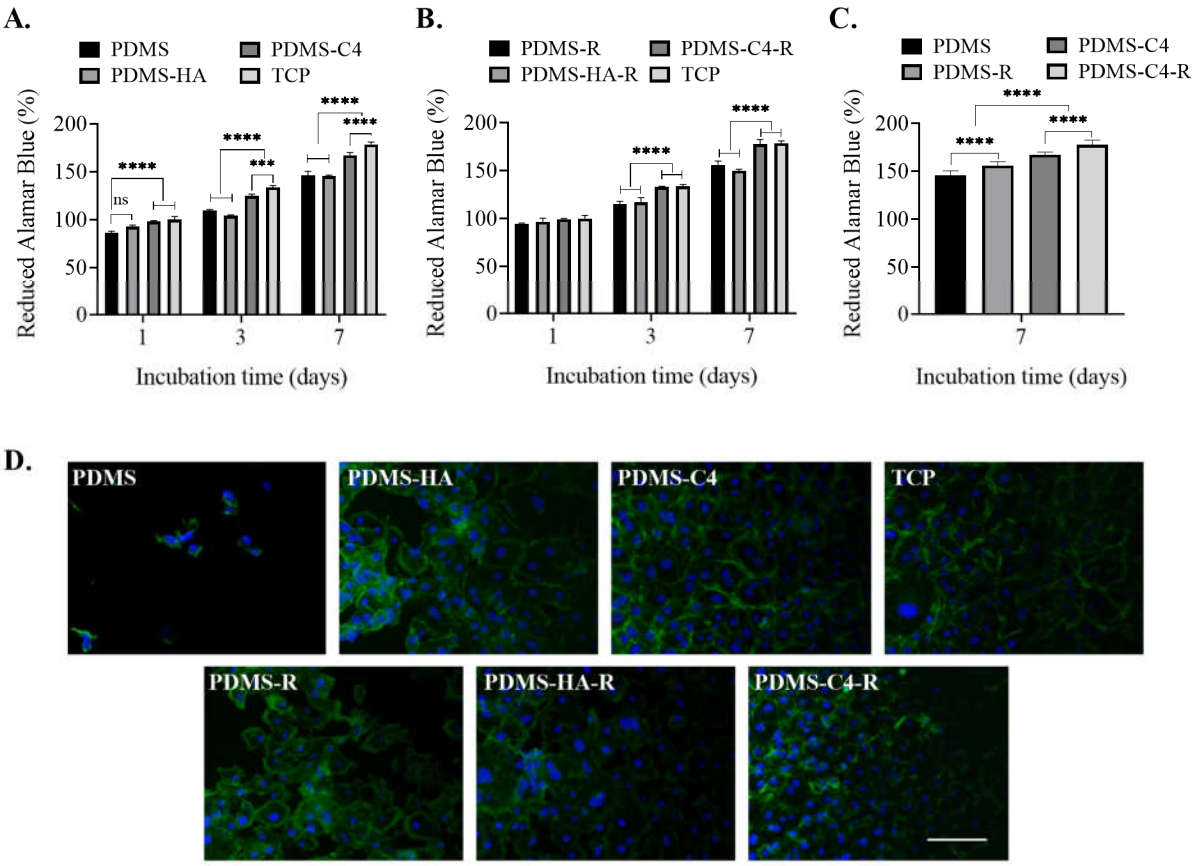

Figure 5. CEC proliferation and morphology on PDMS substrates. Reduced alamar blue (%) with relative CEC proliferation on (A) flat and (B) white rose patterned native PDMS, PDMS-HA, PDMS-C4 and TCP over 7 days and (C) CEC proliferation on flat and white rose patterned PDMS and COL 4 on day 7 (***$p < 0.001$ and ****$p < 0.0001$). (D) Actin cytoskeleton (green) and nuclei (blue) staining of CECs on PDMS substrates (Scale bar = 100 µm).

3.5. Investigation of CEC phenotype

Expression of CEC-relative marker Na^+/K^+ ATPase was investigated (Figure 6) to verify the CEC phenotype via immunofluorescent staining. All experimental groups gave positive signals with varying dispersion. In flat native and HA functionalized PDMS, Na^+/K^+ ATPase signals were not intense, whereas PDMS-C4 provided the highest Na^+/K^+ ATPase activity, including the positive control group-TCP. White rose patterning resulted in an increase of stained areas in all groups. Among patterned substrates, uniform distribution and the highest staining intensity were achieved on PDMS-C4-R with densely populated CECs.

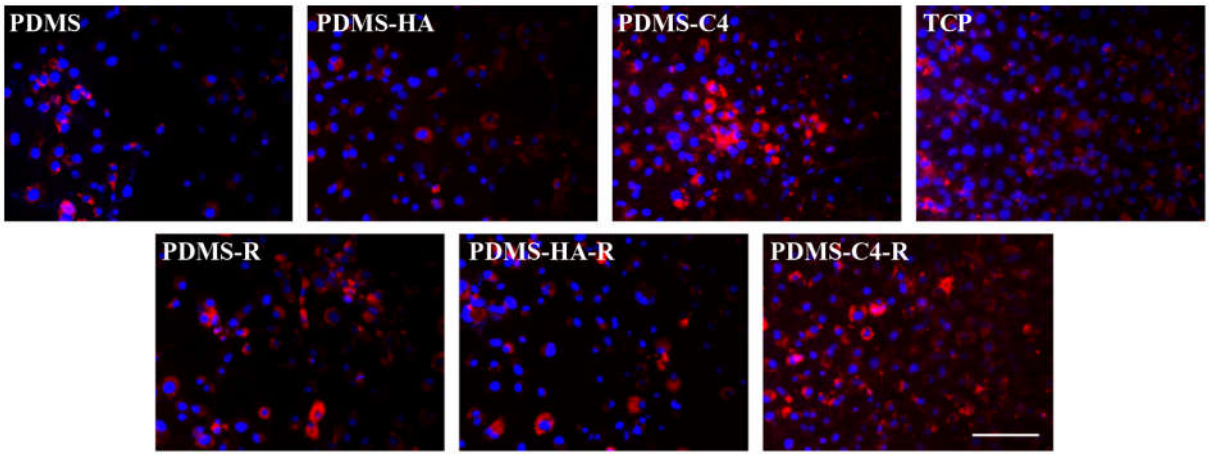

Figure 6. Immunofluorescent staining of CECs for Na^+/K^+ ATPase (red) and DAPI (blue). Scale bar = 100 μm.

Further investigation of CEC phenotype specific markers was conducted with the cell substrates that showed enhanced cell responses in Na^+/K^+ ATPase immunostaining: PDMS-C4, PDMS-C4-R and TCP. Western blot analysis on Figure 7 demonstrated that depositions of CEC-related functional proteins, Na^+/K^+ ATPase, N-Cadherin and Collagen IV were detected on all these substrates with relatively highest expressions on PDMS-C4-R. Confirming immunostaining results, Na^+/K^+ ATPase expression of cells was significantly higher on patterned PDMS-C4, than flat one ($*p < 0.05$), similar to another CEC-specific marker, N-Cadherin. Although PDMS-C4-R group showed the highest expression, the difference between PDMS-C4-R and TCP was not significant for both Na^+/K^+ ATPase and N-Cadherin (Figure 7A-B). However, deposition of Collagen IV was significantly up-regulated on patterned PDMS-C4 than its flat version ($**p < 0.01$) and TCP ($*p < 0.05$). Collagen IV is one the most important ECM components for the maintenance of healthy CEC hexagonal morphology. Increased expression of Collagen IV, in addition to Na^+/K^+ ATPase and N-Cadherin implied that white rose negative relief patterned PDMS substrates enhanced CEC-specific functions, *in vitro*.

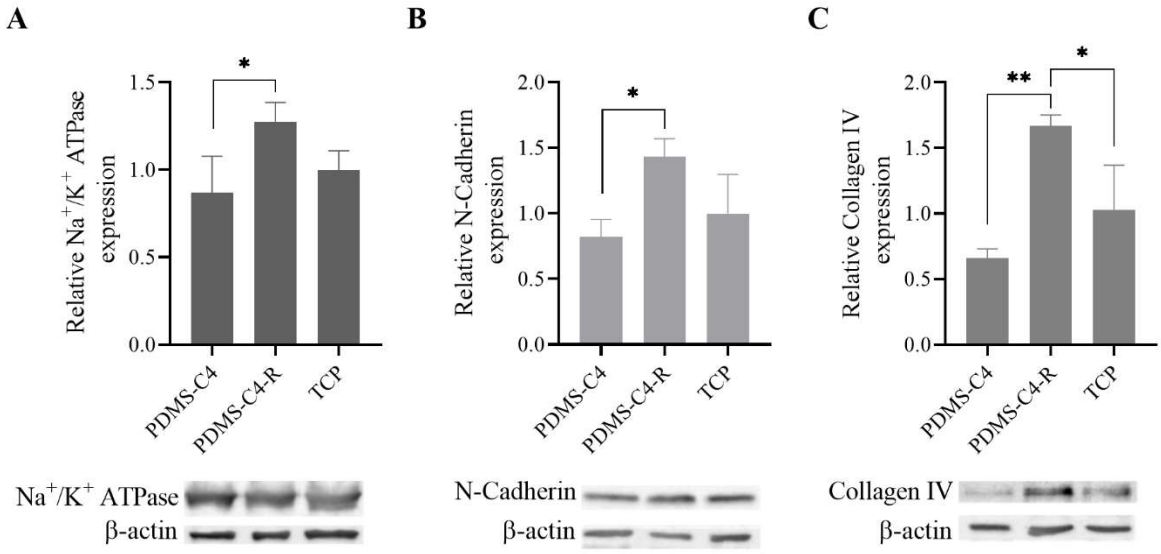

Figure 7. Western blot analysis of CECs on PDMS-C4, PDMS-C4-R and TCP. Quantification of (A) Na^+/K^+ ATPase, (B) N-Cadherin and (C) Collagen IV markers relative to β-actin (*$p < 0.05$ and **$p < 0.01$).

4. Discussion

In this study, we developed biomimetic PDMS cell substrates having a cornea-friendly stiffness, white rose petal negative relief patterned surface topography and corneal ECM-like surface biochemistry. A successful cell substrate should support *in vitro* cell attachment, proliferation and cell type specific functions, as if those cells are at their own *in vivo* environment. Therefore, there is growing interest on preparation of natural cell microenvironment-like substrates having well-regulated mechanical, physical and chemical properties. Here, we focused on CECs, as they are one of the cell types, which cannot regenerate *in vivo* and the decrease in cell number would eventually cause certain diseases and vision loss [1,11]. Keratoplasty has been the main treatment of such corneal endothelial diseases, however due to the limited availability of donor tissues, new approaches are required [49]. The major challenge in the development of alternative methods is the expansion of functional CECs *in vitro*. Production of successful cell substrates for functional CECs proliferation *in vitro* would not only enable treatment opportunities to more patients using lower number of donor corneas, but also would provide an alternative environment to drug design or cell therapy applications. To

address this need, we have developed a cell substrate for *in vitro* CEC culture (PDMS-C4-R) with optimized surface properties.

Micro- to nano-scale topographical features on materials are sensed by cells and modulate their behavior [50,51]. Various cell types, like fibroblasts [52], osteoblasts[53] or MSCs [54], have been investigated to show the effect of substrate surface topography on cell response. Similarly, in corneal regeneration and reconstruction, numerous studies demonstrated the influence of micro- and nanoscale geometrical cues on cell adhesion, maturation, proliferation, morphology or differentiation [55]. Simple pattern cues (grooves, wells, pillars, pits, etc.) have been fabricated for corneal epithelial cells [56], corneal keratinocytes [57], corneal keratocytes [58], corneal stromal cells [59] or CECs [60]. However high precision design considerations on natural microenvironment architecture are required to produce substrate surfaces with enhanced biomimetic topography. In their native microenvironment, CECs are in direct contact with the nanotopography of underlying Descemet's membrane [61]. Inspired by these isotropic cues, micro- and nanoscale pillars and wells were formed on various substrates, like PDMS or TCP, and these patterned substrates provided enhanced CEC proliferation and functional marker expression [12,27,60]. Instead of producing geometrical structures on cell substrates, we took the advantage of naturally occurring nano- and micropatterns with healthy corneal endothelium-like topography: rose petals. Red and white (both in dry and fresh form) rose petal topographies were investigated with SEM after PDMS replication (Figure 3A). Fresh white rose petal mimicked surfaces showed healthy CEC shape-like hexagonal patterns [Figure 3B(i)] [49]. Furthermore, the density of these patterns (≈ 2000 cells/mm^2) was in the physiologically relevant range of corneal endothelium (well above the critical level, which is between 400 – 500 cells/mm^2 [62]), depth of hexagonal shapes (≈ 6.6 μm), were similar to CECs (≈ 5 μm) [42] and nanotopographical cues were naturally formed inside each hexagon [Figure 3A(iii) and Figure 3B(ii)]. SEM images of copies confirmed that a PDMS mold can be used for at least 10 times with excellent pattern fidelity (Figure S2).

For the production of cell substrates, we investigated Young's modulus of PDMS with various base and curing agent ratios, as cells are also responsive to the stiffness of their environment [11,63]. Palchesko et al. confirmed that substrates with Descemet's membrane-like chemo-mechanical properties resulted improved CEC behavior. Among other ECM proteins and

substrates with various stiffness, Collagen IV coated PDMS with an elastic modulus of 50 kPa was found to enhance CEC proliferation (> 3000 fold) and the expression of phenotypic markers [4]. We used 10:1 to 30:1 PDMS base to curing agent ratios in this study and 30:1 PDMS with 211.85±74.9 kPa Young's modulus (Figure 4A) was found in the bulk modulus range of cornea, which is between 200-290 kPa [32,43–45]. All patterned cell substrates were prepared using 30:1, as using PDMS with lower curing agent amounts did not allow successful replication. By adjusting PDMS stiffness to this cornea-friendly range, biomimetic properties of cell substrates were enhanced.

In addition to the optimized topographical and mechanical properties of PDMS substrates, we have also functionalized their surfaces with two corneal ECM components: HA and COL 4. Although patterning resulted a significant increase in CEC proliferation ($p < 0.0001$, Figure 5C) and the number of attached cells (Figure 5D), actin fibers were disrupted on native PDMS and did not provide linking between adjacent cells, revealing the importance of surface chemical modification. Functionalization of PDMS surfaces with HA or COL 4 was completed using NHS/EDC chemistry (Figure 2) and demonstrated by WCA measurements, XPS analysis and immunofluorescent staining (Figure 4B-H). The presence of N-C=O, C=O and the significant increase in C-N and C-C peaks in high resolution C1s spectra of PDMS-HA (Figure 4F) and PDMS-C4 (Figure 4G) indicated that modification was achieved successfully [40,47,64]. Additionally, wettability properties of HA and COL 4 modified PDMS (Figure 4B) were consistent with the literature with hydrophilic PDMS-C4 [65] and relatively hydrophobic nature of PDMS-HA [66]. After successful functionalization of PDMS substrates with these corneal ECM components, proliferation of CECs was enhanced, as seen in Figure 5A-C. This effect was more distinctive in PDMS-C4, as collagen type IV is one of the main constituents of Descemet's membrane [67]. Accordingly, PDMS-C4 successfully mimics the natural microenvironment of CECs. Among all flat PDMS substrates, PDMS-C4 provided the most suitable environment for CEC expansion (Figure 5A), whereas white rose patterning of PDMS-C4 enhanced proliferative capacity of CECs significantly ($p < 0.0001$) and showed similar effects with the control group, TCP (Figure 5B and C). Although HA modification of PDMS did not change CEC metabolic activities, it ensured cellular attachment and better cytoskeleton formation, when compared to native PDMS (Figure 5D). HA is a naturally occurring glycosaminoglycan and known to facilitate cell adhesion [16]. Especially on PDMS-HA-R, cell adhesion was considerably higher,

due to the enhanced biomimetic properties of substrates. However, even flat PDMS-C4 provided better cell adhesion than patterned PDMS-HA, with improved interconnections between cells and increased attached cell number. Moreover, cells on patterned PDMS-C4 showed typical CEC polygonal shapes and formed a confluent cell monolayer, whereas elongated CEC shapes with relatively low number of cells were found on TCP. Actin cytoskeleton staining of CECs on patterned PDMS showed the guidance effect of white rose petal negative relief topography, with enhanced interconnections between adjacent cells and maintenance of uniform hexagonal CEC shape.

The PDMS-C4-R cell substrates were not only effective for *in vitro* CEC proliferation, but also for their physiological functionality. Na^+/K^+ ATPase expression of cells on substrates was investigated to evaluate the activity and vitality of CECs. Localization of Na^+/K^+ ATPase is very crucial for the regulation of corneal pumping function. This pump function prevents stroma from overhydration and maintains optical transparency [68]. Positive immunostaining of Na^+/K^+ ATPase was observed on all substrates (Figure 6); however, the staining intensity was higher in flat and patterned, COL 4 modified PDMS. Teo et al. reported that laminin coated micro- and nanopatterned PDMS with 10:1 base to curing agent ratio enhanced Na^+/K^+ ATPase expression of CECs [27]. Similarly, CECs on micro- and nanoscale patterned TCP showed enhanced functional marker expression [12]. In our study, among all substrates PDMS-C4-R facilitated the highest immunofluorescent intensity against Na^+/K^+ ATPase, whereas both PDMS-C4-R and TCP showed similar CEC proliferation. Western blot analysis confirmed immunostaining results with enhanced CEC phenotype specific marker expressions arising from white rose petal mimicked surface topography (Figure 7). Significantly higher up-regulations of healthy corneal endothelium related morphological and functional proteins of Collagen IV [9], Na^+/K^+ ATPase [69] and N-Cadherin [5] indicated that combination of cornea-friendly substrate stiffness with biomimetic surface chemistry and topography predominates over the positive effects of TCP on CECs and PDMS-C4-R provided functional expansion of CECs.

In conclusion, similarities between white rose petal topography and natural healthy CEC microenvironment have been demonstrated in this study for the first time in the literature. These mimicked micro- and nanoscale architectures were obtained without any need of a donor. Here, we enhanced CEC-substrate characteristics of PDMS, which has been a widely used polymer for

corneal applications, due to its good optical transparency, non-toxicity and biocompatibility, with a biomimetic approach, by optimizing mechanical, topographical and biochemical properties. These substrates would be promising alternatives for *in vitro* CEC expansion and ocular drug investigations.

Declaration of interests

The authors declare that they have no known competing financial interests or personal relationships that could have appeared to influence the work reported in this paper.

Acknowledgments

This study was supported by Bogazici University Research Fund by Grant Numbers 11501 and 6701.

References

[1] Y.T. Tsao, C.M. Cheng, W.C. Wu, H.C. Chen, Bioengineering of Human Corneal Endothelial Cells from Single- to Four-Dimensional Cultures, Curr. Ophthalmol. Rep. (2020). https://doi.org/10.1007/s40135-020-00244-y.

[2] J.A. Sanchis-Gimeno, A. Lleó-Pérez, L. Alonso, M.S. Rahhal, F. Martínez-Soriano, Corneal endothelial cell density decreases with age in emmetropic eyes, Histol. Histopathol. (2005). https://doi.org/10.14670/HH-20.423.

[3] A.E.K. Hutcheon, J.D. Zieske, X. Guo, 3D in vitro model for human corneal endothelial cell maturation, Exp. Eye Res. (2019). https://doi.org/10.1016/j.exer.2019.04.003.

[4] R.N. Palchesko, K.L. Lathrop, J.L. Funderburgh, A.W. Feinberg, In Vitro Expansion of Corneal Endothelial Cells on Biomimetic Substrates, Sci. Rep. (2015). https://doi.org/10.1038/srep07955.

[5] P. Sun, L. Shen, C. Zhang, L. Du, X. Wu, Promoting the expansion and function of human

corneal endothelial cells with an orbital adipose-derived stem cell-conditioned medium, Stem Cell Res. Ther. (2017). https://doi.org/10.1186/s13287-017-0737-5.

[6] B. Van den Bogerd, S.N. Dhubhghaill, C. Koppen, M.J. Tassignon, N. Zakaria, A review of the evidence for in vivo corneal endothelial regeneration, Surv. Ophthalmol. (2018). https://doi.org/10.1016/j.survophthal.2017.07.004.

[7] G.S.L. Peh, R.W. Beuerman, A. Colman, D.T. Tan, J.S. Mehta, Human corneal endothelial cell expansion for corneal endothelium transplantation: An overview, Transplantation. (2011). https://doi.org/10.1097/TP.0b013e3182111f01.

[8] N. Okumura, D. Matsumoto, Y. Fukui, M. Teramoto, H. Imai, T. Kurosawa, T. Shimada, F. Kruse, U. Schlötzer-Schrehardt, S. Kinoshita, N. Koizumi, Feasibility of cell-based therapy combined with descemetorhexis for treating Fuchs endothelial corneal dystrophy in rabbit model, PLoS One. (2018). https://doi.org/10.1371/journal.pone.0191306.

[9] Y.-H. Wang, T.-H. Young, T.-J. Wang, Investigating the effect of chitosan/ polycaprolactone blends in differentiation of corneal endothelial cells and extracellular matrix compositions, Exp. Eye Res. 185 (2019) 107679. https://doi.org/https://doi.org/10.1016/j.exer.2019.05.019.

[10] Z. Chen, X. Liu, J. You, Y. Song, E. Tomaskovic-Crook, G. Sutton, J.M. Crook, G.G. Wallace, Biomimetic corneal stroma using electro-compacted collagen, Acta Biomater. (2020). https://doi.org/10.1016/j.actbio.2020.07.004.

[11] S.S. Mahdavi, M.J. Abdekhodaie, S. Mashayekhan, A. Baradaran-Rafii, A.R. Djalilian, Bioengineering Approaches for Corneal Regenerative Medicine, Tissue Eng. Regen. Med. (2020). https://doi.org/10.1007/s13770-020-00262-8.

[12] R. Muhammad, G.S.L. Peh, K. Adnan, J.B.K. Law, J.S. Mehta, E.K.F. Yim, Micro- and nano-topography to enhance proliferation and sustain functional markers of donor-derived primary human corneal endothelial cells, Acta Biomater. (2015). https://doi.org/10.1016/j.actbio.2015.03.016.

[13] M. Rafat, F. Li, P. Fagerholm, N.S. Lagali, M.A. Watsky, R. Munger, T. Matsuura, M. Griffith, PEG-stabilized carbodiimide crosslinked collagen-chitosan hydrogels for corneal

tissue engineering, Biomaterials. (2008). https://doi.org/10.1016/j.biomaterials.2008.06.017.

[14] T.J. Wang, I.J. Wang, S. Chen, Y.H. Chen, T.H. Young, The phenotypic response of bovine corneal endothelial cells on chitosan/polycaprolactone blends, Colloids Surfaces B Biointerfaces. (2012). https://doi.org/10.1016/j.colsurfb.2011.10.043.

[15] L. Koivusalo, J. Karvinen, E. Sorsa, I. Jönkkäri, J. Väliaho, P. Kallio, T. Ilmarinen, S. Miettinen, H. Skottman, M. Kellomäki, Hydrazone crosslinked hyaluronan-based hydrogels for therapeutic delivery of adipose stem cells to treat corneal defects, Mater. Sci. Eng. C. (2018). https://doi.org/10.1016/j.msec.2017.12.013.

[16] Y. Liu, L. Ren, Y. Wang, Crosslinked collagen-gelatin-hyaluronic acid biomimetic film for cornea tissue engineering applications, Mater. Sci. Eng. C. (2013). https://doi.org/10.1016/j.msec.2012.08.030.

[17] J.H. An, S.Y. Park, G.H. Kim, I.P. Mo, S. Kim, H.M. Woo, K.M. Park, Tissue engineered ultra-thin descemet stripping corneal endothelial layers using porcine cornea and stem cells, Exp. Eye Res. (2020). https://doi.org/10.1016/j.exer.2020.108192.

[18] I.M. El-Sherbiny, M.H. Yacoub, Hydrogel scaffolds for tissue engineering: Progress and challenges, Glob. Cardiol. Sci. Pract. (2013). https://doi.org/10.5339/gcsp.2013.38.

[19] R.M. Alexander, The Gecko's Foot. Bio-Inspiration: Engineered from Nature by Peter Forbes, Nat. (London, United Kingdom). (2005).

[20] Inspired by biology: From molecules to materials to machines, 2008. https://doi.org/10.17226/12159.

[21] N. Suresh Kumar, R. Padma Suvarna, K. Chandra Babu Naidu, P. Banerjee, A. Ratnamala, H. Manjunatha, A review on biological and biomimetic materials and their applications, Appl. Phys. A. 126 (2020) 445. https://doi.org/10.1007/s00339-020-03633-z.

[22] D. Jhala, H. Rather, D. Kedaria, J. Shah, S. Singh, R. Vasita, Biomimetic polycaprolactone-chitosan nanofibrous substrate influenced cell cycle and ECM secretion affect cellular uptake of nanoclusters, Bioact. Mater. (2019). https://doi.org/10.1016/j.bioactmat.2018.12.004.

[23] Y. Liu, H. Gu, Y. Jia, J. Liu, H. Zhang, R. Wang, B. Zhang, H. Zhang, Q. Zhang, Design and preparation of biomimetic polydimethylsiloxane (PDMS) films with superhydrophobic, self-healing and drag reduction properties via replication of shark skin and SI-ATRP, Chem. Eng. J. (2019). https://doi.org/10.1016/j.cej.2018.09.022.

[24] J. Teichmann, M. Valtink, M. Nitschke, S. Gramm, R. Funk, K. Engelmann, C. Werner, Tissue Engineering of the Corneal Endothelium: A Review of Carrier Materials, J. Funct. Biomater. (2013). https://doi.org/10.3390/jfb4040178.

[25] A.J. Engler, C. Carag-Krieger, C.P. Johnson, M. Raab, H.-Y. Tang, D.W. Speicher, J.W. Sanger, J.M. Sanger, D.E. Discher, Embryonic cardiomyocytes beat best on a matrix with heart-like elasticity: scar-like rigidity inhibits beating, J. Cell Sci. (2008). https://doi.org/10.1242/jcs.029678.

[26] A.J. Engler, S. Sen, H.L. Sweeney, D.E. Discher, Matrix Elasticity Directs Stem Cell Lineage Specification, Cell. (2006). https://doi.org/10.1016/j.cell.2006.06.044.

[27] B.K.K. Teo, K.J. Goh, Z.J. Ng, S. Koo, E.K.F. Yim, Functional reconstruction of corneal endothelium using nanotopography for tissue-engineering applications, Acta Biomater. (2012). https://doi.org/10.1016/j.actbio.2012.04.020.

[28] A. Gutermuth, J. Maassen, E. Harnisch, D. Kuhlen, A. Sauer-Budge, C. Skazik-Voogt, K. Engelmann, Descemet's Membrane Biomimetic Microtopography Differentiates Human Mesenchymal Stem Cells into Corneal Endothelial-Like Cells, Cornea. (2019). https://doi.org/10.1097/ICO.0000000000001765.

[29] M.Ö. Öztürk Öncel, B. Garipcan, Stem Cell Behavior on Microenvironment Mimicked Surfaces, Adv. Surfaces Stem Cell Res. (2016) 425–452. https://doi.org/10.1002/9781119242642.ch15.

[30] L. Gitlin, P. Schulze, D. Belder, Rapid replication of master structures by double casting with PDMS, Lab Chip. (2009). https://doi.org/10.1039/b904684d.

[31] M.Ö. Öztürk-Öncel, S. Odabaş, L. Uzun, D. Hür, B. Garipcan, A facile surface modification of poly(dimethylsiloxane) with amino acid conjugated self-assembled monolayers for enhanced osteoblast cell behavior, Colloids Surfaces B Biointerfaces. 196

(2020) 111343. https://doi.org/https://doi.org/10.1016/j.colsurfb.2020.111343.

[32] J.A. Last, S.J. Liliensiek, P.F. Nealey, C.J. Murphy, Determining the mechanical properties of human corneal basement membranes with atomic force microscopy, J. Struct. Biol. 167 (2009) 19–24. https://doi.org/10.1016/j.jsb.2009.03.012.

[33] Y.M. Park, M. Gang, Y.H. Seo, B.H. Kim, Artificial petal surface based on hierarchical micro- and nanostructures, Thin Solid Films. (2011). https://doi.org/10.1016/j.tsf.2011.07.013.

[34] D. Ebert, B. Bhushan, Wear-resistant rose petal-effect surfaces with superhydrophobicity and high droplet adhesion using hydrophobic and hydrophilic nanoparticles, J. Colloid Interface Sci. (2012). https://doi.org/10.1016/j.jcis.2012.06.070.

[35] M. Karaman, N. Çabuk, D. Özyurt, Ö. Köysüren, Self-supporting superhydrophobic thin polymer sheets that mimic the nature's petal effect, Appl. Surf. Sci. (2012). https://doi.org/10.1016/j.apsusc.2012.07.079.

[36] L. Feng, Y. Zhang, J. Xi, Y. Zhu, N. Wang, F. Xia, L. Jiang, Petal effect: A superhydrophobic state with high adhesive force, Langmuir. (2008). https://doi.org/10.1021/la703821h.

[37] J.Y. Lai, Biofunctionalization of gelatin microcarrier with oxidized hyaluronic acid for corneal keratocyte cultivation, Colloids Surfaces B Biointerfaces. (2014). https://doi.org/10.1016/j.colsurfb.2014.07.009.

[38] P.J. Wipff, H. Majd, C. Acharya, L. Buscemi, J.J. Meister, B. Hinz, The covalent attachment of adhesion molecules to silicone membranes for cell stretching applications, Biomaterials. (2009). https://doi.org/10.1016/j.biomaterials.2008.12.022.

[39] Y.J. Chuah, S. Kuddannaya, M.H.A. Lee, Y. Zhang, Y. Kang, The effects of poly(dimethylsiloxane) surface silanization on the mesenchymal stem cell fate, Biomater. Sci. (2015). https://doi.org/10.1039/c4bm00268g.

[40] Z. Yue, X. Liu, P.J. Molino, G.G. Wallace, Bio-functionalisation of polydimethylsiloxane with hyaluronic acid and hyaluronic acid - Collagen conjugate for neural interfacing, Biomaterials. 32 (2011) 4714–4724. https://doi.org/10.1016/j.biomaterials.2011.03.032.

[41] F. Sarvi, Z. Yue, K. Hourigan, M.C. Thompson, P.P.Y. Chan, Surface-functionalization of PDMS for potential micro-bioreactor and embryonic stem cell culture applications, J. Mater. Chem. B. 1 (2013) 987–996. https://doi.org/10.1039/C2TB00019A.

[42] A.O. Eghrari, S.A. Riazuddin, J.D. Gottsch, Overview of the Cornea: Structure, Function, and Development, 1st ed., Elsevier Inc., 2015. https://doi.org/10.1016/bs.pmbts.2015.04.001.

[43] N.E.K. Cartwright, J.R. Tyrer, J. Marshall, Age-related differences in the elasticity of the human cornea, Investig. Ophthalmol. Vis. Sci. (2011). https://doi.org/10.1167/iovs.09-4798.

[44] P.J. Shih, C.J. Huang, T.H. Huang, H.C. Lin, J.Y. Yen, I.J. Wang, H.J. Cao, W.P. Shih, C.A. Dai, Estimation of the Corneal Young's Modulus in Vivo Based on a Fluid-Filled Spherical-Shell Model with Scheimpflug Imaging, J. Ophthalmol. (2017). https://doi.org/10.1155/2017/5410143.

[45] K.E. Hamilton, D.C. Pye, Young's modulus in normal corneas and the effect on applanation tonometry, Optom. Vis. Sci. (2008). https://doi.org/10.1097/OPX.0b013e3181783a70.

[46] A. Scarano, F. Lorusso, T. Orsini, M. Morra, G. Iviglia, L. Valbonetti, Biomimetic surfaces coated with covalently immobilized collagen type I: An x-ray photoelectron spectroscopy, atomic force microscopy, micro-CT and histomorphometrical study in rabbits, Int. J. Mol. Sci. (2019). https://doi.org/10.3390/ijms20030724.

[47] N. Marín-Pareja, E. Salvagni, J. Guillem-Marti, C. Aparicio, M.P. Ginebra, Collagen-functionalised titanium surfaces for biological sealing of dental implants: Effect of immobilisation process on fibroblasts response, Colloids Surfaces B Biointerfaces. (2014). https://doi.org/10.1016/j.colsurfb.2014.07.038.

[48] Z. Qian, D. Ross, W. Jia, Q. Xing, F. Zhao, Bioactive polydimethylsiloxane surface for optimal human mesenchymal stem cell sheet culture, Bioact. Mater. (2018). https://doi.org/10.1016/j.bioactmat.2018.01.005.

[49] M. Parekh, S. Ferrari, C. Sheridan, S. Kaye, S. Ahmad, Concise Review: An Update on

the Culture of Human Corneal Endothelial Cells for Transplantation, Stem Cells Transl. Med. (2016). https://doi.org/10.5966/sctm.2015-0181.

[50] M. Nikkhah, F. Edalat, S. Manoucheri, A. Khademhosseini, Engineering microscale topographies to control the cell-substrate interface, Biomaterials. (2012). https://doi.org/10.1016/j.biomaterials.2012.03.079.

[51] M. Mirbagheri, V. Adibnia, B.R. Hughes, S.D. Waldman, X. Banquy, D.K. Hwang, Advanced cell culture platforms: a growing quest for emulating natural tissues, Mater. Horizons. (2019). https://doi.org/10.1039/c8mh00803e.

[52] V.A. Schulte, M. Díez, M. Möller, M.C. Lensen, Surface topography induces fibroblast adhesion on intrinsically nonadhesive poly(ethylene glycol) substrates, Biomacromolecules. (2009). https://doi.org/10.1021/bm900631s.

[53] J.L. Charest, M.T. Eliason, A.J. García, W.P. King, Combined microscale mechanical topography and chemical patterns on polymer cell culture substrates, Biomaterials. (2006). https://doi.org/10.1016/j.biomaterials.2005.11.022.

[54] R.J. McMurray, N. Gadegaard, P.M. Tsimbouri, K. V. Burgess, L.E. McNamara, R. Tare, K. Murawski, E. Kingham, R.O.C. Oreffo, M.J. Dalby, Nanoscale surfaces for the long-term maintenance of mesenchymal stem cell phenotype and multipotency, Nat. Mater. (2011). https://doi.org/10.1038/nmat3058.

[55] S. Xiong, H.C. Gao, L. Qin, Y.G. Jia, L. Ren, Engineering topography: Effects on corneal cell behavior and integration into corneal tissue engineering, Bioact. Mater. (2019). https://doi.org/10.1016/j.bioactmat.2019.10.001.

[56] S.J. Liliensiek, S. Campbell, P.F. Nealey, C.J. Murphy, The scale of substratum topographic features modulates proliferation of corneal epithelial cells and corneal fibroblasts, J. Biomed. Mater. Res. - Part A. (2006). https://doi.org/10.1002/jbm.a.30744.

[57] P. Eberwein, T. Steinberg, S. Schulz, D. Zimmermann, R. Accardi, D. Beck, T. Reinhard, P. Tomakidi, Expression of keratinocyte biomarkers is governed by environmental biomechanics, Eur. J. Cell Biol. (2011). https://doi.org/10.1016/j.ejcb.2011.08.005.

[58] A.I. Teixeira, P.F. Nealey, C.J. Murphy, Responses of human keratocytes to micro- and

nanostructured substrates, J. Biomed. Mater. Res. - Part A. (2004). https://doi.org/10.1002/jbm.a.30089.

[59] P. Bhattacharjee, B.L. Cavanagh, M. Ahearne, Effect of substrate topography on the regulation of human corneal stromal cells, Colloids Surfaces B Biointerfaces. (2020). https://doi.org/10.1016/j.colsurfb.2020.110971.

[60] S. Koo, R. Muhammad, G.S.L. Peh, J.S. Mehta, E.K.F. Yim, Micro- and nanotopography with extracellular matrix coating modulate human corneal endothelial cell behavior, Acta Biomater. (2014). https://doi.org/10.1016/j.actbio.2014.01.015.

[61] G.A. Abrams, S.S. Schaus, S.L. Goodman, P.F. Nealey, C.J. Murphy, Nanoscale topography of the corneal epithelial basement membrane and Descemet's membrane of the human, Cornea. (2000). https://doi.org/10.1097/00003226-200001000-00012.

[62] J. Zavala, G. Ló Pez Jaime, C.R. Barrientos, J. Valdez-Garcia, Corneal endothelium: developmental strategies for regeneration, Eye. 27 (2013) 579–588. https://doi.org/10.1038/eye.2013.15.

[63] R. Chen, L. Li, L. Feng, Y. Luo, M. Xu, K.W. Leong, R. Yao, Biomaterial-assisted scalable cell production for cell therapy, Biomaterials. (2020). https://doi.org/10.1016/j.biomaterials.2019.119627.

[64] M. Morra, C. Cassinelli, G. Cascardo, P. Cahalan, L. Cahalan, M. Fini, R. Giardino, Surface engineering of titanium by collagen immobilization. Surface characterization and in vitro and in vivo studies, Biomaterials. (2003). https://doi.org/10.1016/S0142-9612(03)00360-0.

[65] C. Li, Y. Ding, S. Kuddannaya, Y. Zhang, L. Yang, Anti-bacterial properties of collagen-coated glass and polydimethylsiloxane substrates, J. Mater. Sci. (2017). https://doi.org/10.1007/s10853-017-1175-6.

[66] P. Xue, Q. Li, Y. Li, L. Sun, L. Zhang, Z. Xu, Y. Kang, Surface modification of poly(dimethylsiloxane) with polydopamine and hyaluronic acid to enhance hemocompatibility for potential applications in medical implants or devices, ACS Appl. Mater. Interfaces. (2017). https://doi.org/10.1021/acsami.7b10260.

[67] S. Ponce Márquez, V.S. Martínez, W. McIntosh Ambrose, J. Wang, N.G. Gantxegui, O. Schein, J. Elisseeff, Decellularization of bovine corneas for tissue engineering applications, Acta Biomater. (2009). https://doi.org/10.1016/j.actbio.2009.02.011.

[68] J.A. Bonanno, Molecular mechanisms underlying the corneal endothelial pump, Exp. Eye Res. (2012). https://doi.org/10.1016/j.exer.2011.06.004.

[69] Y.J. Hsueh, D.H.K. Ma, K.S.C. Ma, T.K. Wang, C.H. Chou, C.C. Lin, M.C. Huang, L.J. Luo, J.Y. Lai, H.C. Chen, Extracellular matrix protein coating of processed fish scales improves human corneal endothelial cell adhesion and proliferation, Transl. Vis. Sci. Technol. (2019). https://doi.org/10.1167/tvst.8.3.27.

[70] M. Teferra, Poly-dimethylsiloxane (PDMS) an ideal biomaterial for cornea replacement, Int. J. Latest Res. Eng. Technol. 3 (2017) 77–82.